Available online at www.sciencedirect.com

ScienceDirect

Procedia Engineering 10 (2011) 3668–3676

Engineering Procedia

ICM11

The Influence of Hydrogen on Thermal Desorption Processes in Structural Materials

R. Bar[b], E. Dabah[a], D. Eliezer[b], Th. Kannengiesser[a], Th. Boellinghaus[a]

[a] **BAM, Federal Institute for Materials Research and Testing, Berlin Germany**

[b] **Ben-Gurion University of the Negev, Department of Materials Engineering, Beer Sheva Israel**

Abstract

Hydrogen embrittlement is a form of environmentally assisted failure caused by the action of hydrogen, often in combination with residual or applied stress that results in a reduction in the load-bearing capacity of a component. It was found that hydrogen has a direct influence on the lattice parameter and on the thermal expansion characteristic. Hydrogen's desorption behavior in this process and its effects on the mechanical behavior of those materials are discussed in detail.

Keywords: hydrogen embrittlement; hydrogen desorption; LDS; SMSS

1. Introduction

In this research a thermal desorption process was carried out in order to observe the influence of hydrogen upon the lattice in that specific process. Lattice distortions, such as planar spacing expansion, have been monitored during the thermal desorption process and are correlated to the dissolved hydrogen in the different alloys. In this research, two alloys, lean duplex stainless steel (LDS) and super martensite stainless steel (SMSS) were examined and a comparison was made between them.

LDS is a recently developed low-alloyed (lean) DSS with a very similar microstructure to that of the DSS, meaning it has a mixed crystal structure of ferrite (BCC) and austenite (FCC). But it is unique in that it has a different quantity of the alloying elements, granting it better mechanical properties at a reduced cost [3]. The LDS provides high yield strength and has excellent chloride stress corrosion cracking resistance [4].

Super martensite stainless steel, the "super" grades, is composed of ~11% chromium [5]. These steel are in use mainly in the petrochemical and petroleum industries [6]. Several experimental methods are discussed in regards to their applicability as tools for investigating potential hydrogen traps for both alloys and to characterize the physical nature of hydrogen traps. Thermal desorption spectrometry functions as an effective method for the identification of different types of trapping sites and for the

 doi:10.1016/j.proeng.2011.04.604

measurement of their binding energy and density. In addition, an in situ investigation of the kinetics and dynamics of the hydrogen interaction with the crystal lattice was performed by means of X-ray measurements, using the synchrotron at the BESSY-Energy Dispersive Diffraction (EDDI) beam line. Further methods include OM, SEM and other hydrogen measurements.

The aim of this study is to describe the influences of thermal desorption spectroscopy experiments upon the crystal structure of the material, and to be able to explain the diffusion behavior of hydrogen during this kind of experiment.

2. Experimental Procedure

The Lean duplex stainless steel and Super martensitic stainless steel were received as a plate with a thickness of 1mm, in a fully annealed condition. The compositions of these alloys were valuated by means of chemical measurements, and are presented in Table 1.

Table 1

Chemical composition of the investigated LDS and SMSS (%wt.)

Sample	C	S	P	Mn	Si	Ni	Cr	Mo	N	Cu
LDS 2101	0.026	0.001	0.025	4.9	0.63	1.53	21.53	0.2	0.22	0.28
SMSS	**0.063**	**0.002**	**0.021**	**1.859**	**0.364**	**7.002**	**10.513**	**3.315**	**0.009**	**0.467**

The hydrogenation process was performed using electrochemical cathodic charging.
The characteristics of hydrogen desorption were investigated by means of thermal desorption spectrometry. The technique involves accurate measurement of the desorption rate of gas atoms, either solute or trapped in the material, while heating the sample at a known rate of under UHV ~10μpa. The samples were heated from R.T. to 450^{o}C at a constant heating rate of 2, 4 and 6^{o}C/sec. The total amount of hydrogen absorbed into the samples as a result of the electrochemical charging process and the amount of retained hydrogen after thermal desorption, were estimated by way of LECO RH-404.
The microstructure, phase composition and lattice parameter of the stainless steel specimens were examined, before and after hydrogenation, by means of a Rigaku Type D/max-2100 X-Ray diffractometer with nickel-filtered Cu-Kα radiation (λ=1.54Å), in the range of $30<2\theta<90$ and by means of an Energy Dispersive Diffraction (EDDI) beamline at the synchrotron facilities of the Helmholtz Zentrum Berlin(HZB–BESSY).

The beamline EDDI creates white synchrotron radiation with energy values ranging from 0 to 120keV. The wide X-ray energy range makes it possible to keep the reflection angle at a constant position of 6◦. These parameters provide the conditions needed for a wide diffraction spectrum within a very short time of10s. The performed measurements allow for in situ observations of diffractogram modifications caused by hydrogen during a period of 24h at an ambient temperature. The charged specimens were aged at room temperature and were examined at different time increments in order to observe the different phase transformations during hydrogen desorption.

3. Results and Discussion

3.1. Hydrogen-induced structure transformation

X- ray diffractions were carried out and the results showed similar intensities in the γ and α phases, indicating an approximately 50-50 percent ferrite- austenite structure in the LDS sample. Furthermore, aging at R.T. after cathodic charging showed that hydrogen had a significant affect during the austenitic phase rather than in the ferittic phase. New reflections observed for the specimens after hydrogen charging and outgassing can be indexed as belonging to the ε martensite and γ* pseudo hydride phases. The γ* and the γ-austenitie reflections are overlapping and their lattice parameters are fairly equal during the various aging times. Moreover the amount of ε decreased upon aging, reaching a steady amount after longer aging times. This is due to the ε lattice parameters, which after longer aging times approached those of ε martensite formed by plastic deformation. This suggests that the ε phase that is formed by hydrogen charging continuously transforms to the hydrogen-free ε phase.

The microstructure of the SMSS consists mainly of BCT structure and small amounts of retained austenite (~15%). These observations are in line with the XRD spectra, which showed only two phases: the residual γ phase and the α martensite phase with a BCT structure.

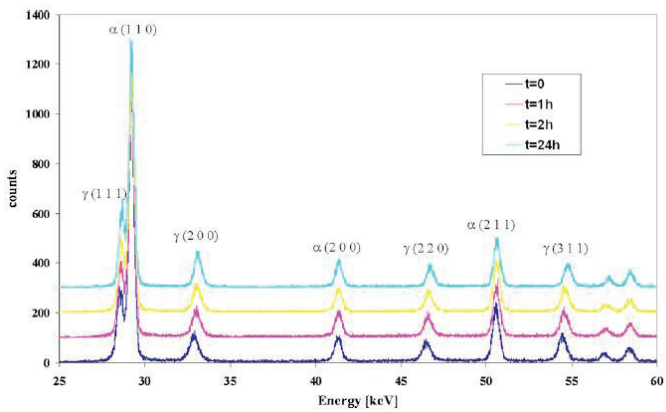

Fig. 1. Energy Dispersive Diffractograms taken at different times during hydrogen effusion [7]

Aging after cathodic charging of the SMSS is presented in Fig 1. The obtained diffractograms taken at different time intervals demonstrates a slight shift of the diffraction peaks towards higher energy levels with increasing aging times. These changes can only be observed in the austenite phase. Changes were not found in the BCT (α') peaks.

The extraction of the peak's accurate positions were performed by fitting the diffractograms to the Gaussian function and then converting them to inter planar spacing according to Bragg's Law. These values have been assigned to Figs. 2 and 3 for the fcc (γ) and the BCT (α'), respectively.

The large scattering in the positions are typical and are attributed to fitting errors and an inexact match of the diffraction curve to the Gaussian function. However, such diagrams clearly exhibit the changes in the lattice spacing, based on the shift in the reflection position. It becomes clear by such analysis procedure that the position of the reflection shifts to higher energy values with time. According to Bragg's Law, higher energy values correspond to smaller interplanar spacing and thus, it can be seen from such diagrams that the plane spacing decreases with time for one single reason, i.e. hydrogen evolution. The increased interplanar spacing of the hydrogen charged samples, observed during the initial stage of the

measurement, can be attributed to the hydrogen dissolved in the metal matrix. With a presumed linear relationship between hydrogen content and lattice expansion, the contraction of the lattice as a result of hydrogen effusion shows a steep slope in the beginning of the process, which then moderates with further hydrogen desorption. This is an indication of the dependence of the desorption rate on the hydrogen concentration gradient. The larger the solute hydrogen concentration, the higher the desorption rate [7].

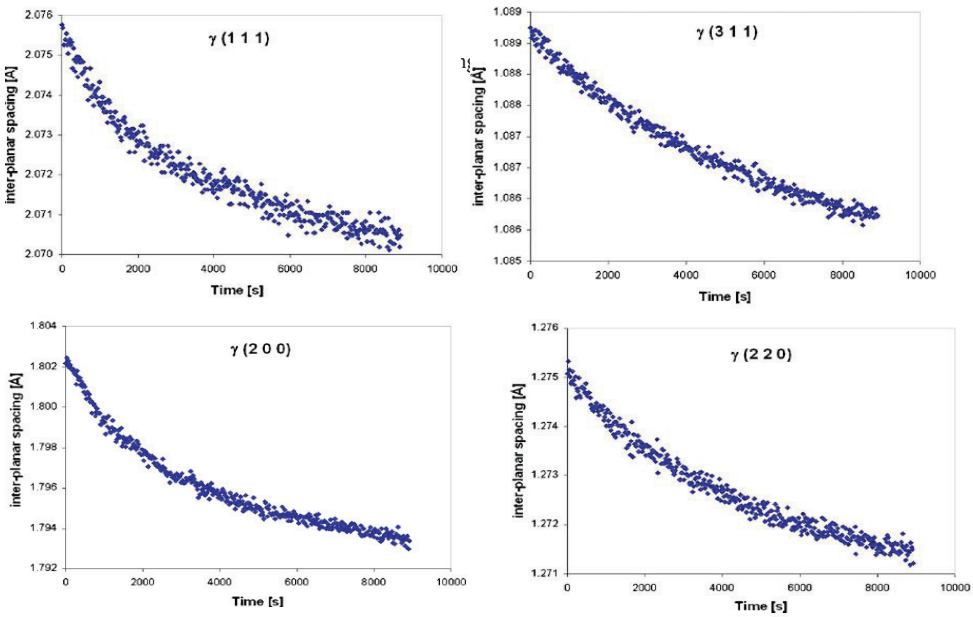

Fig. 2. Changing of the planar lattice spacing correlated to austenite phase reflections [7]

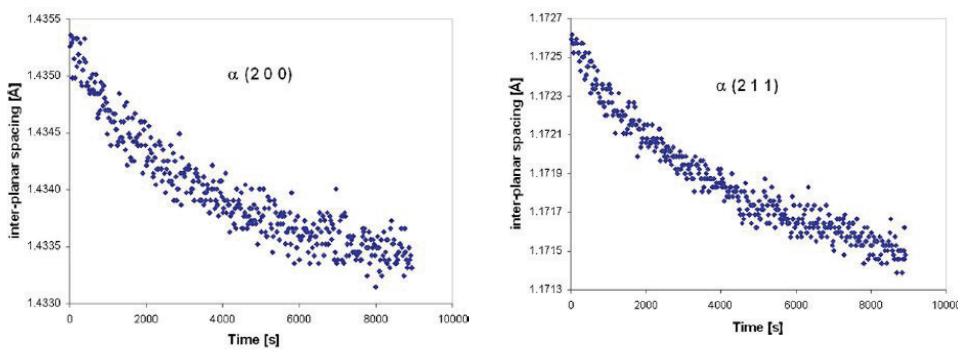

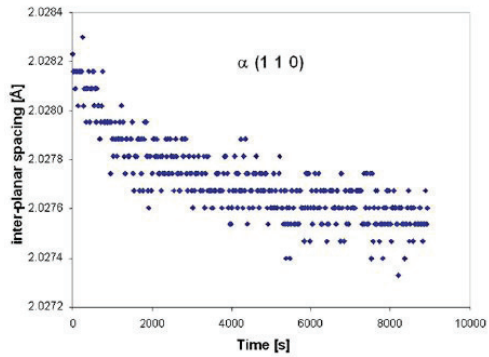

Fig. 3. Changing of the planar lattice spacing correlated to martensite phase reflections [7]

The SEM results of the LDS fractography show both facet cleavage fracture in the ferritic phase and cleavage fracture associated with plastic deformation in the austenitic phase. The cracking path of hydrogen is a typical brittle cleavage in the ferritic phase, which then induces a microcrack in the austenitic grain crossing the ferritic–austenitic boundary. Finally, the crack propagates throughout the austenitic grain.

The fractography of the SMSS did not reveal any significant changes – only a few microcracks on the surface. The cracks appear to be intergranular. These results can be explained as demonstrating relatively low hydrogen solubility within the SMSS grains, which leads to a lower hydrogen concentration, therefore not inducing severe stress.

3.2. Thermal Desorption Spectra

The TDS spectra of the SMSS and the LDS are presented in Figs 4 and 6. All samples were heated from R.T. to 450^{o}C using heating rates of 2, 4, and 6^{o}C/sec. For the experiment, samples were chosen after a hydrogenation process of 24h and 72h.

All TDS spectra show a singular peak at low temperatures, which characterizes hydrogen desorption from the surface of the sample, followed by a series of peaks at higher temperatures and lower intensities, which characterize hydrogen desorption from the bulk. It can be observed that all plots have 3 main peaks. When heating rates are increased the peaks move to higher intensities and experience a shift in temperature. By referencing the shift of desorption peak temperatures in connection with varying heating rates, the activation energy for hydrogen desorption from a particular trap can be calculated. The activation energy was calculated by applying Lee and Lee's model [8,9] and is presented in Figs 5 and 7.

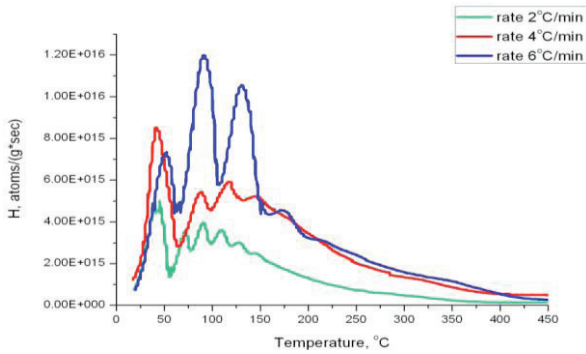

Fig. 4. TDS spectra of LDS after charging with hydrogen for 72h

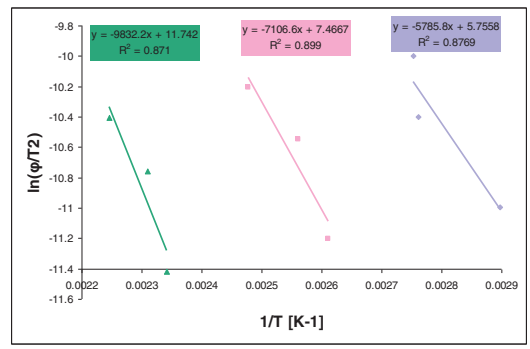

Fig. 5. Applying Lee and Lee's model for activation energy calculation for LDS, charged for 72h

Table 2

Activation energies calculated for LDS

24 hours		72 hours	
Temperature [ºC]	Eact [KJ/mol]	Temperature [ºC]	Eact [KJ/mol]
82-106	42	72-90	48
102-125	51	110-131	59
130-150	61	154-172	82

Our results as described in Table 2 and Table 3 are in agreement with previously published findings [5, 6]. The traps activation energy for 24h and 72h hydrogenation are between 42-82kj/mole which is in accordance with reversible traps energies such as dislocation (20-30kj/mole), grain boundary (18-59kj/mole) and vacancies (38-48kj/mole). This indicates that those traps can be identified as reversible traps. By assuming that the thermal desorbed hydrogen is only from reversible traps as can be seen from Table 2, the retained hydrogen in the irrversible traps can be calculated by subtraction of the activation energy results (from TDS) from the LECO results (Table 6).

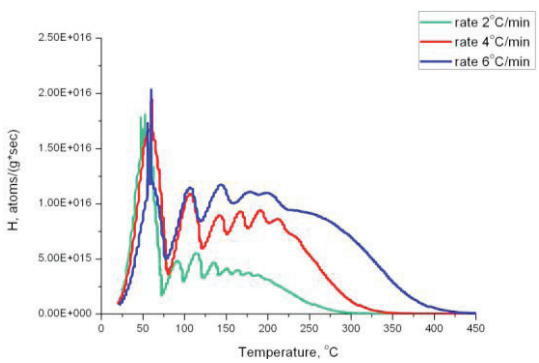

Fig. 6. TDS spectra of SMSS after charging with hydrogen for 72 h

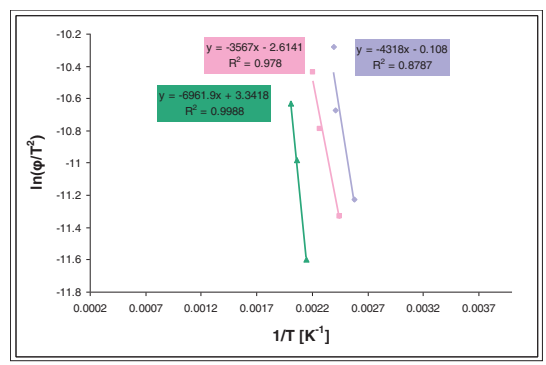

Fig. 7. Applying Lee and Lee's model for activation energy calculation for SMSS, charged for 72h

Table 3

Activation energies calculated for SMSS

24 hours		72 hours	
Temperature [ºC]	Eact [KJ/mol]	Temperature [ºC]	Eact [KJ/mol]
95-140	23	115-145	35
117-167	24	135-180	30
197-205	29	193-226	56

Table 4

Total amount of thermal desorbed hydrogen for LDS and SMSS

sample	24 hours Charging time		72 hours Charging time	
	Heating Rate [ºC/min]	Calculated Desorbed Hydrogen [ppm]	Heating Rate [ºC/min]	Calculated Desorbed Hydrogen [ppm]
LDS	2	13	2	28.1
	4	16.7	4	29.2
	6	12.2	6	23.5
SMSS	2	12.1	2	43.8
	4	13.5	4	48
	6	24.3	6	47

Table 5

Retained hydrogen from irreversible traps for LDS and SMSS

Sample	24 hours Charging time		72 hours Charging time	
	Total absorbed Hydrogen [ppm]	Estimated residual Hydrogen after thermal desorption [ppm]	Total absorbed Hydrogen [ppm]	Estimated residual Hydrogen after thermal desorption [ppm]
LDS	242.5	~229	390	~363
SMSS	405	~379	630	~583

It can be observed from Tables 4 and 5, that the majority of desorbed hydrogen is located in the irreversible traps. Only a small amount of the desorbed hydrogen (~14ppm within 24h hydrogenation and ~27ppm within 72h hydrogenation) is located in the reversible traps.

Our assessment, which is consistent with other published results [12], is that reversible traps will exchange hydrogen with stronger traps, thereby acting as hydrogen sources. Irreversible traps are so strong as to not release hydrogen at all. Therefore irreversible hydrogen traps will carry more hydrogen.

Conclusions

- Higher stability of γ* and ε reflections are caused by a less stable γ phase, which is due to lower austenite stabilizer.
- After longer aging times the ε lattice parameters in the LDS consistently approached those of the ε martensite formed by plastic deformation and changes to the hydrogen-free ε phase.
- The SMSS shows higher resistance to hydrogen embrittlement (a few microcracks), due to higher hydrogen solubility.
- The absorption capability is more dependent on hydrogen diffusion rather than on solubility.
- The traps activation energy is in accordance with reversible traps energies such as dislocation, grain boundary or vacancies.
- The majority of desorbed hydrogen is located in the irreversible traps.
- By measuring the changes in the lattice parameter according to Bragg's law, the effects of hydrogenation on both phases ,i.e. fcc (γ) austenite and the bcc (α') martensite, and the kinetics of hydrogen desorption at room temperature can be clearly observed in in situ energy dispersive diffraction measurements taken using hard synchrotron radiation.
- Hydrogen causes reversible lattice expansion in the respective fcc (γ) austenite and bcc (α') martensite phases, which regains its original dimensions after the hydrogen is desorbed. At ambient temperature, most of the hydrogen dissolved in the lattice during the two phases evolves within a time period of less than 24 h.
- Consistent with other published findings, hydrogen solution in the austenite phase is associated with larger lattice expansion, which indicates that it has higher solubility than the martensite phase.

References

[1] Davis J.R, ASM Specialty Handbook, Stainless Steel, 3rd ed., Ohio: ASM International;1999.
[2] C. D. Beachem, Metallurgical Transactions 1972; **3**: 1972-437.
[3] Sieurin H., Sandstorm R. and Westin E.M., Metallurgical and MaterialsTransaction A 2006; **37A:** 2975-81.
[4] I. Avarez-Armas, Journal of Mechanical Engineering 2008; **1**:51-57.
[5] Lacombe P., Baroux B., Beranger G., Stainless Steels, Les Editions De Physique Les Ulis;1993.
[6] ASTM: designation: E 975- 95
[7] E. Dabah, Th. Kannengiesser, D. Eliezer and Th. Boellinghaus, Materials Science and Engineering A 2011; **528**:1608–14.
[8] Ch. Genzel et al, Nuclear Instruments and Methods in Physics Research A 2007; **578**: 23–33.
[9] Lee S.M and Lee J.Y, Metallurgical and Materials Transactions A 1986; **17A**:181-7.
[10] E. Dabah,V.Lisitsyn, D.Eliezer, Materials Science and Engineering: A 2010;**527**: 4851–57.
[11] D.Eliezer, E.Tal-Gutelmacher, C.Cross, Th.Boellinghaus, Materials Science and Engineering: A 2006;**421**:200–7.
[12] G.M Pressouyre, Acta Metallurgica1980; **28**:895.
[13] N. Narita, C. J. Altstetter and H. K. Birnbaum, Metallurgical Transactions A, Aug. 1982;**13A**:1355
[14] Chou. Sh-L and Tsai. W-T., Materials Science and Engineering A 1999;**270**: 219–24.
[15] V. Di Cocco, E. Franzese et al., Engineering Fracture Mechanics 2008;**75**:705–14.